Neutron diffraction reveals sequence-specific membrane insertion of pre-fibrillar islet amyloid polypeptide and inhibition by rifampicin

Neutron diffraction reveals sequence-specific membrane insertion of pre-fibrillar islet amyloid polypeptide and inhibition by rifampicin

Kia Balali-Mood[a], Richard H. Ashley[b], Thomas Haußc, Jeremy P. Bradshaw[a,*]

[a] *Veterinary Biomedical Sciences, R.(D.)S.V.S., University of Edinburgh, Summerhall, Edinburgh EH9 1QH, UK*
[b] *Biomedical Sciences, University of Edinburgh Medical School, George Square, Edinburgh EH8 9XD, UK*
[c] *Hahn-Meitner-Institut, Glienicker Straße 100, D-14109 Berlin, Germany*

Received 30 August 2004; revised 8 November 2004; accepted 23 December 2004

Available online 19 January 2005

Edited by Irmgard Sinning

Abstract Human islet amyloid polypeptide (hIAPP) forms amyloid deposits in non-insulin-dependent diabetes mellitus (NIDDM). Pre-fibrillar hIAPP oligomers (in contrast to monomeric IAPP or mature fibrils) increase membrane permeability, suggesting an important role in the disease. In the first structural study of membrane-associated hIAPP, lamellar neutron diffraction shows that oligomeric hIAPP inserts into phospholipid bilayers, and extends across the membrane. Rifampicin, which inhibits hIAPP-induced membrane permeabilisation in functional studies, prevents membrane insertion. In contrast, rat IAPP (84% identical to hIAPP, but non-amyloidogenic) does not insert into bilayers. Our findings are consistent with the hypothesis that membrane-active pre-fibrillar hIAPP oligomers insert into beta cell membranes in NIDDM.

Keywords: Alzheimer's disease; Diabetes mellitus; Ion channel; Non-insulin-dependent diabetes mellitus; Phospholipid bilayer

1. Introduction

A number of extracellular proteins can misfold spontaneously and aggregate to form β-sheet rich amyloid deposits characteristic of a variety of ''protein misfolding'' diseases, most notably Alzheimer's disease [1,2]. While the precise molecular basis of such conditions is unclear, strong arguments are emerging to implicate organ-specific amyloidogenic proteins, particularly oligomeric intermediates on the pathway to amyloid fibril formation, in disease pathogenesis (e.g. [3]).

Human islet amyloid polypeptide (hIAPP), a 37-residue peptide hormone secreted by pancreatic beta cells, often forms amyloid deposits in patients affected by NIDDM (non-insulin dependent or type 2, maturity onset, diabetes mellitus). We recently demonstrated that an intermediate, non-fibrillar, oligomeric form of hIAPP interacts with membranes, whereas fibrillar hIAPP (like normal, monomeric hIAPP) lacks membrane activity [4]. Interestingly, the membrane activity of hIAPP could be inhibited independently of its ability to form amyloid [5]. These Langmuir balance measurements provided a further test of the idea that only the pre-fibrillar, oligomeric form of hIAPP is membrane-active, and mature fibrils are inert. Oligomeric intermediates in the 'misfolding' process may form non-specific cation channels [6], and cellular Ca^{2+}-overload could account for the toxicity of hIAPP [7], and explain why exposed cells die by both apoptosis and necrosis [4].

Unlike hIAPP, rat IAPP (rIAPP) is inert [4]. Sequence variations in IAPP are strongly associated with the ability of the peptide to form amyloid, and susceptibility to NIDDM [8,9]. Human and cat IAPP contain the internal sequence NFGAIL (Fig. 1), and both species can form islet amyloid and develop NIDDM. The rat and mouse genes do not encode this motif, and these species do not exhibit islet amyloid or NIDDM. However, mice expressing the hIAPP transgene do develop a NIDDM-like disease [10].

The membrane-active form of hIAPP is currently poorly defined. In the present study, we identified the membrane-associated form of hIAPP in stacked phospholipid bilayers using neutron diffraction. In order to mimic, as closely as possible, the experimental conditions of our previous studies [4,5] the lipid system for this work was a 50:50 mixture of palmitoyl-oleoyl phosphatidylethanolamine (POPE) and palmitoyl-oleoyl phosphatidylserine (POPS). We directly tested the hypothesis that hIAPP oligomers span the bilayer, and our findings are consistent with the idea that oligomeric hIAPP is associated with the formation of transmembrane channels. rIAPP was excluded from the membrane, as predicted, and rifampicin, an inhibitor of the membrane activity of hIAPP [5], prevents membrane insertion.

2. Materials and methods

2.1. Materials

hIAPP and rIAPP were obtained from Bachem (Weil am Rhein, Germany). POPE and POPS were purchased from Avanti Polar Lipids (Birmingham, AL) and rifampicin was from Fluka (Poole, UK). Other chemicals were of the highest purity available.

2.2. Sample preparation and data collection

Multibilayer stacks of phospholipids and peptides were prepared as described previously [11]. Briefly, 20 mg of a 50:50 (mol) mixture of POPE and POPS were co-dissolved with 1% (mol) peptide in chloroform:trifluoroethanol (7:3, v/v) and airbrushed onto a quartz glass slide to produce highly aligned stacks of some 50 000 or so bilayers. Where rifampicin was required in a sample, this was added to the lipid mixture before the peptide. The wafers were placed under vacuum for 24 h to remove the solvents before being mounted in sealed sample cans and hydrated for 12 h at 25 °C to allow full equilibration and the formation of IAPP oligomers [4,5]. The sample cans contained

*Corresponding author. Fax: +44 131 650 6139.
E-mail address: j.bradshaw@ed.ac.uk (J.P. Bradshaw).

0014-5793/$30.00
doi:10.1016/j.febslet.2004.12.085

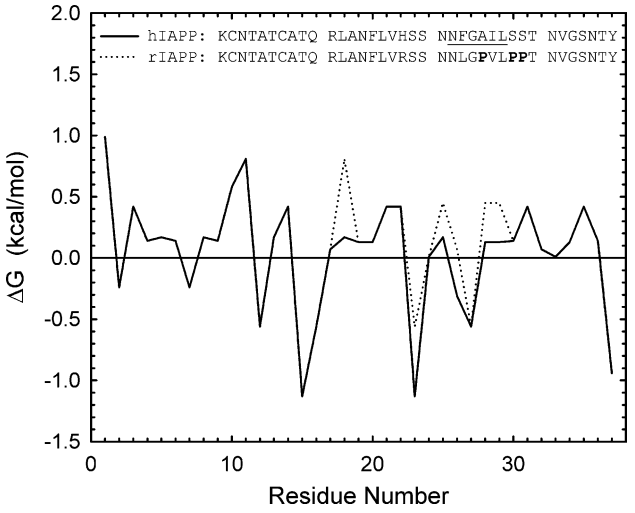

Fig. 1. Hydrophobicity plot of hIAPP (Swiss-Prot P10997) and rIAPP (Swiss-Prot P12969), using the whole residue hydrophobicity scale of Wimley and White [25]. The inset shows a sequence alignment of the two peptides. Each peptide has a disulfide-bridged loop at its N-terminal end. The NFGAIL motif, present in species susceptible to islet amyloid and NIDDM, is underlined. The three prolines present in rat but not hIAPP are indicated in bold.

saturated solutions of KCl, K_2NO_3 or K_2SO_4 in $^2H_2O/H_2O$ mixtures to maintain a relative humidity of 85%, 92% or 97%, respectively, and the ^2H_2O concentration was set to 8% (v/v) in the presence of each of the three salts, and also to 20% (v/v) and 50% (v/v) in K_2NO_3 alone. Diffraction data sets, comprising five orders of diffraction, were collected for each of the five conditions on V1 at the Berlin Neutron-Scattering Center, Hahn-Meitner-Institut, Berlin, Germany, by scanning samples through ±2° around the predicted Bragg angle for each of the first five orders of diffraction in turn.

2.3. Data analysis

After background subtraction, peak fitting and absorption and Lorentz corrections, the intensities were square-rooted to provide structure factor amplitudes. Phasing the structure factors is a two stage process. In the first, the three sets of 8% ^2H_2O structure factors are fitted to a single continuous transform, thereby fixing their phases [11]. In the second, the 8% ^2H_2O phases are used as a basis for phasing the data collected at 20% and 50% ^2H_2O by least-squares fitting to straight line functions, as described previously [12]. This two-step approach has the added advantage that an accurate set of 8% ^2H_2O structure factors can be calculated from first stage for increased accuracy in the second. The data were then placed on a 'relative absolute' scale using the method of White and co-workers [13]. In this approach, the data are placed on an absolute scale using the known neutron scattering lengths of all component molecules. However, since the x and y dimensions are not probed by lamellar diffraction methods, these two dimensions are not specified in the treatment of the data. The structure factor data, and the profiles calculated from them are, therefore, scaled to represent a single pair of lipids plus the appropriate number of water and peptide molecules. At 1% (mol) peptide, the unit cell in this study represents two lipid molecules and 0.02 molecules of peptide.

3. Results

3.1. Lamellar d-repeats

The lamellar spacings (d-repeats) of the samples at 92% relative humidity were determined by optimised least squares fitting to five orders of diffraction. 1% (mol) hIAPP decreased the lamellar spacing significantly from 62.09 ± 0.16 Å (means ± S.D., $n = 3$) to 61.51 ± 0.20 Å (means + S.D., $n = 3$, $P < 0.02$ by t-testing), while rIAPP increased the spacing slightly to 62.72 ± 0.57 Å ($n = 3$, $P > 0.05$). The measurements for phospholipids with 1% (mol) rifampicin were 56.96 ± 0.43 Å (means ± S.D., $n = 3$), and for phospholipids with 1% (mol) hIAPP and 1% (mol) rifampicin, 58.53 ± 0.27 Å (means ± S.D., $n = 3$). The difference in d-repeats between bilayers containing hIAPP and rIAPP (in the absence of rifampicin) is 1.2 Å. Assuming an average bilayer surface area of 72 $Å^2$ per phospholipid [14], this difference equates to a volume increase of 87 $Å^3$ per pair of lipids (the basis of the 'relative absolute' scaling method). The total molecular volume of IAPP calculated from amino acid volumes in the IMB Jena Image Library (http://www.imb-jena.de) is 4680 $Å^3$. At 1% (mol), this equates to an extra volume of 47 $Å^3$ per lipid, or 94 $Å^3$ per pair of lipids.

The additional volume of the peptide could be accommodated either by expansion of the unit cell in the Z-direction (e.g., if the long axis of the peptide lies parallel to the bilayer), or by insertion of hIAPP between the bilayer phospholipids, or both. The significant decrease in the d-repeat in the presence of hIAPP was inconsistent with the first possibility. However, expansion of the unit cell in the plane of the bilayer, the second possibility, is invisible to lamellar diffraction methods, and is not constrained in the '*relative* absolute' method used in this study. Moreover, the idea that the peptide inserted into the bilayer was consistent with the monolayer expansion seen in previous Langmuir balance measurements using the same lipids [5]. We therefore investigated the possible membrane insertion of hIAPP in more detail, by examining bilayer scattering profiles.

3.2. Bilayer profiles

The neutron scattering length density profile of POPE/POPS bilayers in the absence of peptide (Fig. 2(a)) differs from the "standard" profile of dioleoylphosphatidylcholine (DOPC) [11], most noticeably because the dip in scattering length density seen in the water region of DOPC bilayer profiles is barely visible in the POPE/POPS profile. This can be explained by the different neutron scattering lengths of the phospholipid headgroups. The total scattering length of the PC ($C_5H_{13}N$), PE (C_2H_7N) and PS ($C_3H_6O_2N$) headgroups are -0.60×10^{-13} cm, -0.597×10^{-13} cm and 1.85×10^{-13} cm, respectively. When two sodium counter ions are added to the PS headgroup (0.72×10^{-13} cm), the extra density in the mixed lipid bilayers is readily explained.

The bilayer profile in the presence of hIAPP (Fig. 2(b)) was remarkably similar to that of pure lipid bilayers. The total neutron scattering length per peptide molecule is 98.78×10^{-12} cm (hIAPP) or 98.51×10^{-12} cm (rIAPP). The water region was almost indistinguishable from the pure phospholipid bilayer, and any relatively slight differences were largely confined to an increase in density in the fatty-acyl region. rIAPP, on the other hand, caused major changes to the water region (Fig. 2(c)). The characteristic minimum at the edges of the profile were completely absent, suggesting that the additional neutron scattering length density introduced by the peptide now filled this trough. The profile shape changes in the fatty acyl-region were consistent with lipid rearrangements rather than peptide penetration. A peptide orientated parallel to the bilayer is likely to cause greater fatty-acyl disruption than a transbilayer peptide, for two reasons: (i) the parallel peptide will have contacts with a much larger number of phospholipids than a transbilayer peptide and (ii) the parallel peptide only occupies part

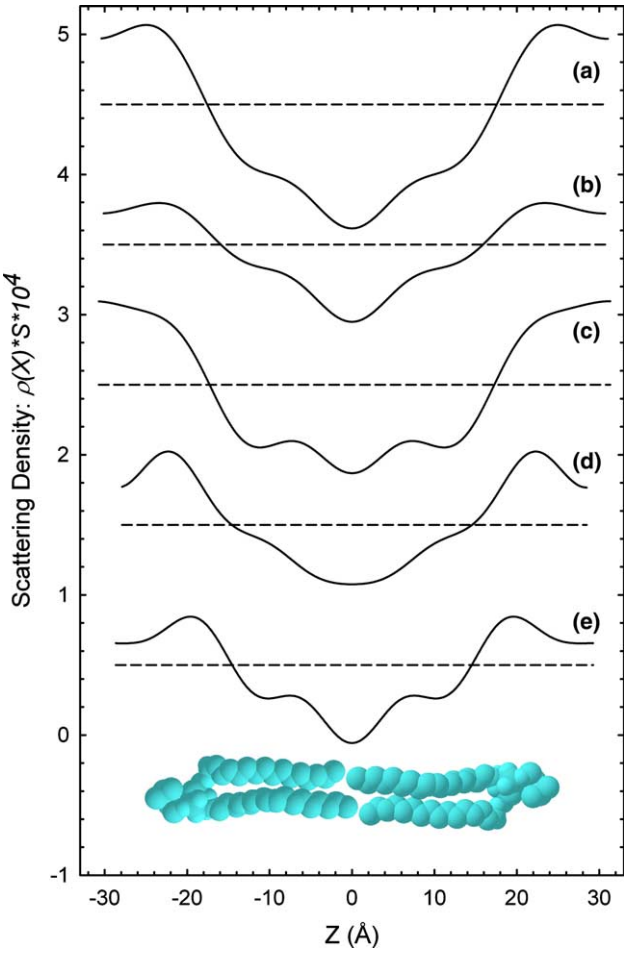

Fig. 2. Neutron scattering length density profiles of phospholipid bilayers: (a) 50:50 (mol) mixture of POPE and POPS; (b) 50:50 (mol) mixture of POPE and POPS with 1% (mol) hIAPP; (c) 50:50 (mol) mixture of POPE and POPS with 1% (mol) rIAPP; (d) 50:50 (mol) mixture of POPE and POPS with 1% (mol) rifampicin; (e) 50:50 (mol) mixture of POPE and POPS with 1% (mol) hIAPP and 1% (mol) rifampicin hIAPP. The structure factors for bilayers hydrated with 8% ^2H_2O were used to calculate the profiles, since water of this isotopic composition has a net neutron scattering length density of zero. The profiles have been displaced vertically, for clarity. A pair of lipid molecules is also shown, for orientation.

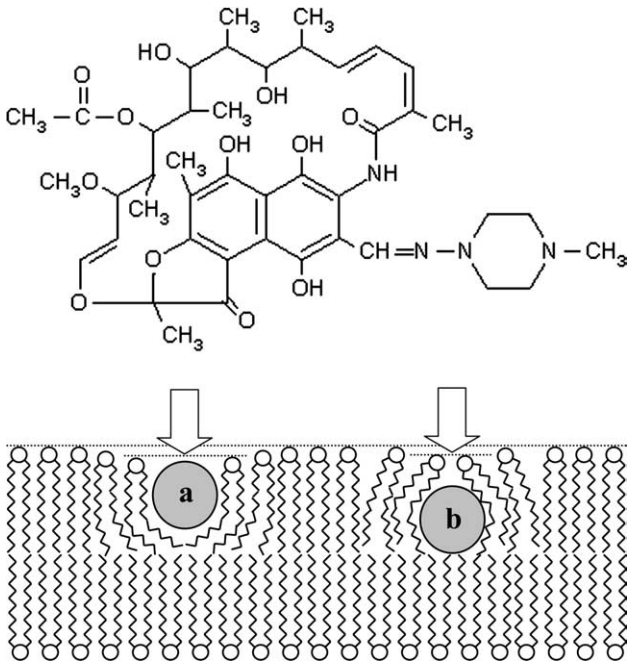

Fig. 3. Top: the structure of rifampicin. Bottom: Cartoon showing possible mechanism of bilayer thinning (arrow) when (a) a peptide inserts parallel to the bilayer surface or (b) rifampicin inserts close to the terminal methyl groups. For explanation, see text.

of the full depth of the bilayer, and will create a potential void that has to be filled by the fatty-acyl chains of the surrounding lipids (Fig. 3(a)). A similar effect has been observed in another interfacial peptide, the antimicrobial peptide protegrin-1 [15]. An alternative mechanism of bilayer thinning is based on the observation that an incorporated molecule may alter the thermal fluctuations which, in turn, can affect the inter-bilayer distance [16].

Taken together, these profiles show clear differences in the relationship of the two peptides with the lipid bilayer. rIAPP appears to reside exclusively in the water layer between the bilayers, whereas hIAPP is largely excluded from this region. This conclusion is further supported by the observation (Figs. 2(a) and (c)) that the bilayers are thinner in the presence of rIAPP, despite the overall increase in *d*-repeat. In profile (a), the two maxima in the neutron scattering length density are caused by strong neutron scattering by the phosphates and the oxygen rich (and hydrogen-poor) ester linkages of the phospholipids. Although partially obscured by scattering from the peptide, the steep gradients up towards the corresponding region are closer together in profile (c) compared to (a).

We next examined how the inhibitor rifampicin interacted with phospholipid bilayers in the absence of peptide. The total neutron scattering length per rifampicin molecule is 18.67×10^{-12} cm. Previous studies of rifampicin partitioning using derivative spectrophotometry [17] and ^{1}H NMR and fluorescence energy transfer [18] suggested that the compound inserts deeply into the hydrophobic core of the bilayer, while remaining in contact with the polar surface. With a pK_a of 7.9, rifampicin has partial anionic character at neutral pH, and this has been correlated with a stronger interaction with zwitterionic lipids such as di-myristoyl phosphatidylcholine ($K_d = 5.09 \times 10^4$) compared to anionic lipids such as di-myristoyl phosphatidylglycerol ($K_d = 0.54 \times 10^4$) [18]. While in broad agreement that rifampicin forms stable bilayers with anionic or zwitterionic lipids, our neutron data reveal that rifampicin induces marked structural changes in the membrane (the NMR technique used by Rodrigues [18] is blind to the details of bilayer structure revealed by neutron diffraction).

In particular, the bilayer profiles in Figs. 2(a) and (d) show differences in bilayer width, as revealed by the distance between the two maxima, and the bilayer thinning caused by rifampicin is reflected in the reduced *d*-repeat of the corresponding samples. These effects may be explained by "splaying" of the phospholipid headgroup regions over the top of deeply inserted rifampicin (Fig. 3(b)). Rodrigues also positions rifampicin close to the terminal methyls of the fatty-acyl chains [18], consistent with our observation that the methyl trough is broadened, as revealed by the neutron

scattering length density at the centre of the bilayer. Addition of hIAPP to the bilayers in the presence of rifampicin thins the bilayer even further, yet increases the *d*-repeat by 1.5 Å. Both of these observations are consistent with location of the peptide to the water/bilayer interfacial region, strongly implying that rifampicin has prevented transbilayer insertion of the peptide.

3.3. The distribution of water

Water distribution profiles were calculated by Fourier transformations of difference structure factor profiles obtained by least-squares fitting to 8%, 20% and 50% ^2H_2O sample hydrations. The water profile for pure lipid bilayers, shown in Fig. 4(a), was entirely consistent with previous neutron studies of phospholipid membranes. The single peak (split between the two ends of the profile in the figure) represents a block of water confined between adjacent bilayers in the multi-bilayer stack. The peak can be fitted (in reciprocal space) to a single pair of Gaussians, centred at 27.8(6) Å from the middle of the bilayer and 5.8(2) Å wide (full width at 1/*e* height).

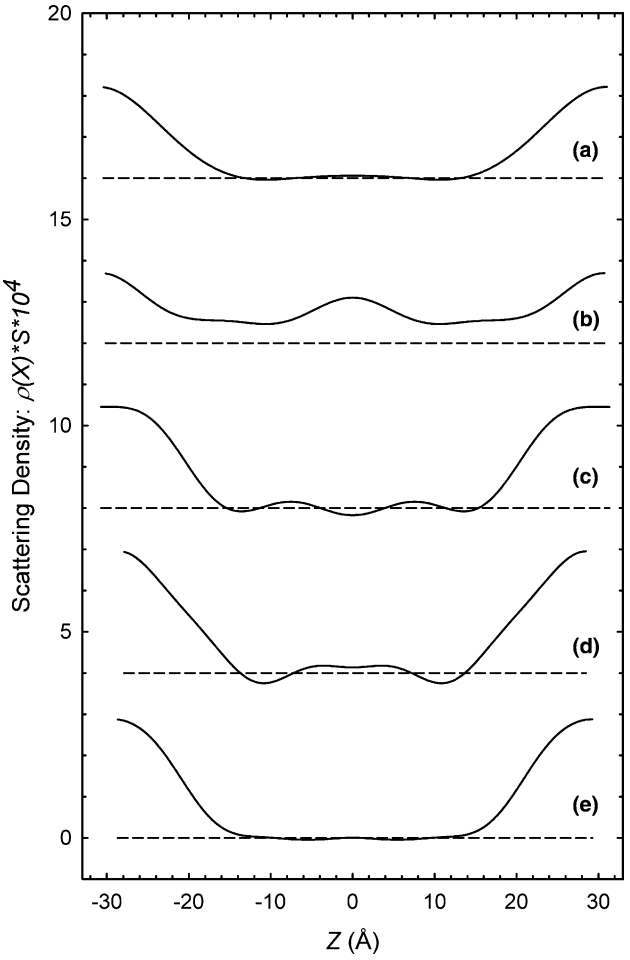

Fig. 4. Difference profiles of the neutron scattering length density of water (^2H_2O) in stacked phospholipid bilayers: (a) 50:50 (mol) mixture of POPE and POPS; (b) 50:50 (mol) mixture of POPE and POPS with 1% (mol) hIAPP; (c) 50:50 (mol) mixture of POPE and POPS with 1% (mol) rIAPP; (d) 50:50 (mol) mixture of POPE and POPS with 1% (mol) rifampicin; (e) 50:50 (mol) mixture of POPE and POPS with 1% (mol) hIAPP and 1% (mol) rifampicin hIAPP. Structure factors for bilayers hydrated in 100% H_2O were subtracted from corresponding 50% ^2H_2O structure factors and the result used to calculate the profiles shown. The profiles have been displaced vertically, for clarity.

The corresponding water distribution profile for bilayers containing 1% (mol) rIAPP (Fig. 4(c)) was similar. Once again, the water was confined to the outer sections of the profile, representing the inter-bilayer hydration layer. This block of neutron scattering length density was fitted (in reciprocal space) to a pair of Gaussians, centred 27.1(1) Å from the middle of the bilayer, and 4.2(5) Å wide. However, in the IAPP profiles (Fig. 4(b)), the same amount of water was distributed very differently. Instead of being confined to the edges, it extended across the entire width of the repeating unit, including the phospholipid bilayer itself. The area under the central portion of this curve corresponds to around 500 deuterons per peptide, comprising water and exchanged protons. This indicates the presence of channel-structures, though the neutron data do not supply any information on the number of peptides per channel. This observation supports the proposal that hIAPP, but not rIAPP, inserts in a transbilayer orientation in the phospholipid bilayers used in this study.

In contrast, in POPC/POPS bilayers with 1% (mol) rifampicin (Fig. 4(d)), the water was largely confined to the inter-bilayer region, and as previously noted, the lipid profile differed in shape (cf. Fig. 4(a)). This confirms the suggestion that rifampicin and phospholipids form stable bilayers, but refutes the claim [18] that the bilayer structure remains unchanged. Of particular interest is the observation that the addition of rifampicin to bilayers containing hIAPP (Fig. 4(e)) constrained the deuterons to the inter-bilayer region, in contrast to appearances in the absence of rifampicin (Fig. 4(b)). However, it is known from functional studies that rifampicin prevents bilayer insertion of hIAPP, rather than blocking pre-inserted "channels" [5].

4. Discussion

In the absence of high-resolution structural data, we have speculated that membrane-active IAPP is a misfolded, β-sheet-rich, primary nucleation element on the amyloid pathway that can insert spontaneously into membranes [5]. Membrane-located IAPP may then refold to give rise to transmembrane α-helices surrounding a central ion channel or pore [5,6]. In this respect, IAPP may follow the pattern displayed by calcitonin (CT), an amyloid-forming peptide that has previously been studied in detail. CT is a 32-amino acid polypeptide hormone that shows sequence and charge distribution similarities to IAPP and can adopt either α- or β-structures, depending on its environment. The former is seen in phospholipid membranes [19], while the latter predominates in aqueous solution [20]. Using methods similar to those in the present study, Bradshaw [19] showed that salmon CT could insert into phospholipid bilayers containing the anionic lipid phosphatidylglycerol, leading to speculation that the peptide may have ion-channel properties. This was later confirmed by Stipani et al. [21]. Human CT formed channels at the same concentration, but not as easily as salmon CT, an observation the authors attributed to the reduced helical content of this form of the peptide.

One possible concern is that, over the several hours of a neutron experiment, the amyloid-forming proteins may form fibrils. However, the neutron data describe highly ordered systems, that do not change over the duration of the neutron measurements. This is consistent with our previous lipid bilayer work [4] and Langmuir balance work [5] that demonstrated that the mature fibril for of IAPP is not membrane-active. Furthermore, it is simply not known whether fibrils can form from peptide that has already inserted into a membrane. The transconformational changes involved in morphing from a structure optimised for a hydrophobic membrane environment to the cross-β amyloid structure could be considerably greater than those involved in adopting the amyloid conformation from aqueous solution.

Fig. 1 shows a hydrophobicity plot for the two peptides. rIAPP is clearly less hydrophobic than hAIPP, a fact which may contribute to the latter's inability to insert into phospholipid bilayers. However, peptide insertion into bilayers also requires the formation of secondary structure and the sequence differences between the two forms of IAPP will have a significant effect on rIAPP's ability to form this structure. The main differences between the sequences of hIAPP and rIAPP are the replacement of the alanine at position 35, and the serines at positions 38 and 39, with proline residues. The first of these replacements disrupts the NFGAIL sequence linked to the formation of islet amyloid and susceptibility to NIDDM [8,9]. Proline is a well-established ''breaker'' of both α-helix and β-sheet structures in globular proteins, because the closed loop structure of the side chain prevents the peptide backbone from adopting the φ and ψ angles required for either of these secondary structures. However, proline frequently occurs in the transmembrane helices of integral membrane proteins, particularly transport proteins, despite the fact that a kink is introduced wherever a proline residue interrupts a helical section. Li and Derber [22] resolved this apparent contradiction by postulating different rules governing structure in the hydrophobic environment of membranes, and showed that the helical propensity of proline was greatly enhanced in the membrane-mimetic environments of both lipid micelles and organic solvents. In studies of a proline to alanine replacement in a single-spanning membrane protein of bacteriophage IKe, Li and Derber [22] showed that proline does not interfere with helix formation, but does prevent the formation of β-sheet. The intrinsic capacity of proline to disrupt β-structures has also been demonstrated by showing that prolines are excluded from transmembrane β-strands in mutagenised OmpA porins that retain the ability to assemble into a membrane-spanning β-barrel [23]. Wigley et al. [24] has proposed that the abundance of proline in transmembrane helices can be entirely explained by the ability of the residue to block β-structures. The advantage conferred by preventing the formation of a β-sheet outweighs the entropic disadvantage in helix distortion.

In this context, it is instructive to consider the differences in sequence, amyloidogenicity and membrane-associated neutron scattering profiles of hIAPP and rIAPP. Following the arguments outlined above, it is tempting to suggest that rIAPP is non-amyloidogenic because the introduction of a proline into the NFGAIL sequence prevents the peptide from adopting the β-structure necessary for amyloid fibre formation. However, this should not significantly interfere with the peptide's ability to insert into phospholipid membranes, if the membrane-active form is α-helical (like the model for CT). Previous studies, and our current neutron diffraction data, indicate that this is not so. Rats are not susceptible to ''NIDDM'', and the neutron data suggest that rIAPP does not insert into phospholipid membranes.

This could be taken as evidence that the membrane-active form of hIAPP is not α-helical, until it is remembered that rIAPP possesses not one but three extra prolines. The disruptive effect of three prolines in close proximity (two of them consecutive residues) is likely to block the formation of both α- and β-structures by the peptide. In the future work, it will clearly be of interest to probe the secondary, tertiary and quaternary structure of membrane-associated hIAPP in detail.

In conclusion, our data represent the first study of membrane-associated IAPP to use diffraction-based techniques. We have shown that oligomeric hIAPP interacts with phospholipid membranes to form transbilayer structures. rIAPP is excluded from the membrane (as predicted), and the insertion of hIAPP is inhibited by rifampicin.

Acknowledgements: We thank the Alzheimer's Research Trust and the University of Edinburgh Development Trust for support.

References

[1] Bucciantini, M., Giannoni, E., Chiti, F., Baroni, F., Formigli, L., Zurdo, J., Taddei, N., Ramponi, G., Dobson, C.M. and Stefani, M. (2002) Inherent toxicity of aggregates implies a common mechanism for protein misfolding diseases. Nature 416, 507–511.
[2] Ellis, R.J. and Pinheiro, T.J.T. (2002) Danger – misfolding proteins. Nature 416, 483–484.
[3] Walsh, D.M., Klyubin, I., Fadeeva, J.V., Cullen, W.K., Anwyl, R., Wolfe, M.S., Rowan, M.J. and Selkoe, D.J. (2002) Naturally secreted oligomers of amyloid beta protein potently inhibit hippocampal long-term potentiation in vivo. Nature 416, 535–539.
[4] Janson, J., Ashley, R.H., Harrison, D., McIntyre, S. and Butler, P.C. (1999) The mechanism of islet amyloid polypeptide toxicity is membrane disruption by intermediate-sized toxic amyloid particles. Diabetes 48, 491–498.
[5] Harroun, T.A., Bradshaw, J.P. and Ashley, R.H. (2001) Inhibitors can arrest the membrane activity of human islet amyloid polypeptide independently of amyloid formation. FEBS Lett. 507, 200–204.
[6] Mirzabekov, T.A., Lin, M.C. and Kagan, B.L. (1996) Pore formation by the cytotoxic islet amyloid peptide amylin. J. Biol. Chem. 271, 1988–1992.
[7] Kelly, J.W. (1998) The alternative conformations of amyloidogenic proteins and their multi-step assembly pathways. Curr. Opin. Struct. Biol. 8, 101–106.
[8] Westermark, P., Engstrom, U., Johnson, K.H., Westermark, G.T. and Betsholtz, C. (1990) Islet amyloid polypeptide – pinpointing amino-acid-residues linked to amyloid fibril formation. Proc. Natl. Acad. Sci. USA 87, 5036–5040.
[9] Tenidis, K., Waldner, M., Bernhagen, J., Fischle, W., Bergmann, M., Weber, M., Merkle, M.L., Voelter, W., Brunner, H. and Kapurniotu, A. (2000) Identification of a penta- and hexapeptide of islet amyloid polypeptide (IAPP) with amyloidogenic and cytotoxic properties. J. Mol. Biol. 295, 1055–1071.
[10] Janson, J., Soeller, W.C., Roche, P.C., Nelson, R.T., Torchia, A.J., Kreutter, D.K. and Butler, P.C. (1996) Spontaneous diabetes mellitus in transgenic mice expressing human islet amyloid polypeptide. Proc. Natl. Acad. Sci. USA 93, 7283–7288.
[11] Darkes, M.J.M. and Bradshaw, J.P. (2000) Real-time swelling series method improves the accuracy of lamellar neutron diffraction data. Acta Crystallogr. D 56, 48–54.
[12] Duff, K.C., Gilchrist, P.J., Saxena, A.M. and Bradshaw, J.P. (1994) Neutron diffraction reveals the site of amantadine

blockade in the influenza A M2 ion channel. Virology 202, 287–293.
[13] Wiener, M.C., King, G.I. and White, S.H. (1991) Structure of a fluid dioleoylphosphatidylcholine bilayer determined by joint refinement of X-ray and neutron-diffraction data. 1. scaling of neutron data and the distributions of double-bonds and water. Biophys. J. 60, 568–576.
[14] Tristram-Nagle, S., Petrache, H.I. and Nagle, J.F. (1998) Structure and interactions of fully hydrated dioleoylphosphatidylcholine bilayers. Biophys. J. 75, 917–925.
[15] Heller, W.T., Waring, A.J., Lehrer, R.I., Harroun, T.A., Weiss, T.M., Yang, L. and Huang, H.W. (2000) Membrane thinning effect of the beta-sheet antimicrobial protegrin. Biochemistry 39, 139–145.
[16] McIntosh, T.J., Magid, A.D. and Simon, S.A. (1989) Cholesterol modifies the short-range repulsive interactions between phosphatidylcholine membranes. Biochemistry 28, 17–25.
[17] Rodrigues, C., Gameiro, P., Reis, S., Lima, J.L.F.C. and Castro, B. (2001) de Derivative spectrophotometry as a tool for the determination of drug partition coefficients in water/dimyristoyl-L-α-phosphatidylglycerol (DMPG) liposomes. Biophys. Chem. 94, 97–106.
[18] Rodrigues, C., Gameiro, P., Prieto, M. and Castro, B. (2003) de Interaction of rifampicin and isoniazid with large unilamellar liposomes: spectroscopic location studies. Biophys. Biochim. Acta 1620, 151–159.
[19] Bradshaw, J.P. (1997) Phosphatidyl glycerol promotes bilayer insertion of salmon calcitonin. Biophys. J. 72, 2180–2186.
[20] Gilchrist, P.J. and Bradshaw, J.P. (1993) Amyloid formation by salmon calcitonin. Biochim. Biophys. Acta 1182, 111–114.
[21] Stipani, V., Gallucci, E., Micelli, S., Picciarelli, V. and Benz, R. (2001) Channel formation by salmon and human calcitonin in black lipid membranes. Biophys. J. 81, 3332–3338.
[22] Li, S.C. and Deber, C.M. (1994) A measure of helical propensity for amino-acids in membrane environments. Nat. Struct. Biol. 1, 368–373.
[23] Koebnik, R. (1999) Membrane assembly of the *Escherichia coli* outer membrane protein OmpA: exploring sequence constraints on transmembrane beta-strands. J. Mol. Biol. 285, 1801–1810.
[24] Wigley, W.C., Corboy, M.J., Cutler, T.D., Thibodeau, P.H., Oldan, J., Lee, M.G., Rizo, J., Hunt, J.F. and Thomas, P.J. (2002) A protein sequence that can encode native structure by disfavoring alternate conformations. Nat. Struct. Biol. 9, 381–388.
[25] Wimley, W.C. and White, S.H. (1996) Experimentally determined hydrophobicity scale for proteins at membrane interfaces. Nat. Struct. Biol. 3, 842–848.